Sensor and Simulation Notes
Note 80
31 March 1969

# The Circular Parallel-Plate Dipole

Capt Carl E. Baum
Air Force Weapons Laboratory

## Abstract

One of the common sensors for measuring an electric field is a dipole with two parallel conducting plates. In this note we consider the case of two equal coaxial conducting plates. The upper frequency response is considered for a special direction of wave incidence; for well designed output circuitry the upper frequency response is not limited by the plate size but by the smaller dimensions associated with the output circuitry. The sensor capacitance is calculated by a numerical solution of an integral equation. Finally we consider the distortion of the electric field produced by a spherical dielectric shell which might be used to enclose the sensor.

## I. Introduction

A parallel-plate dipole is a common sensor for measuring a component of an electric field because of its accurately calculable equivalent height. Such a sensor consists of two thin parallel plates with some device (typically with high impedance) which converts the voltage between the two plates into an analog electrical signal for recording and/or further processing.

In this note we consider some of the characteristics of a symmetrical parallel-plate dipole consisting of two coaxial circular disks of radius a and spacing 2b as illustrated in figure 1. The axis of the plates is taken as the z axis and the plates are located on $z = \pm b$. Because of symmetry in z the present calculations also apply to the case with a perfectly conducting sheet on the plane $z = 0$, provided appropriate factors of two are introduced. For most of the discussion the plates are assumed to have zero thickness.

First we consider the equivalent height of the sensor and some of the associated high-frequency performance characteristics of the sensor. This is followed by calculation of the sensor capacitance. For these considerations the medium in the vicinity of the sensor is assumed isotropic and homogeneous. Then we consider the distortion of an incident field produced by a thin spherical dielectric shell surrounding the sensor. Such a shell might be used for mechanical protection of the sensor and/or for containing a material (such as a special gas) with higher dielectric strength than the surrounding medium.

## II. Equivalent Height and Related Considerations

One of the attractive features of the parallel-plate dipole is its calculable equivalent height. If we ignore the thickness of the plates and the connections to remove the signal then, referring to figure 1, the equivalent height is just[1]

$$\vec{h}_{eq} = 2b\vec{e}_z \tag{1}$$

where $\vec{e}_z$ denotes a unit vector in the z direction (and similarly for other coordinates). Note that we take the upper plate at $z = b$ for our positive voltage convention. The open circuit voltage for a given incident electric field $\vec{E}_{inc}$ is just

$$V_{oc} = -\vec{E}_{inc} \cdot \vec{h}_{eq} \tag{2}$$

1. All units are rationalized MKSA.

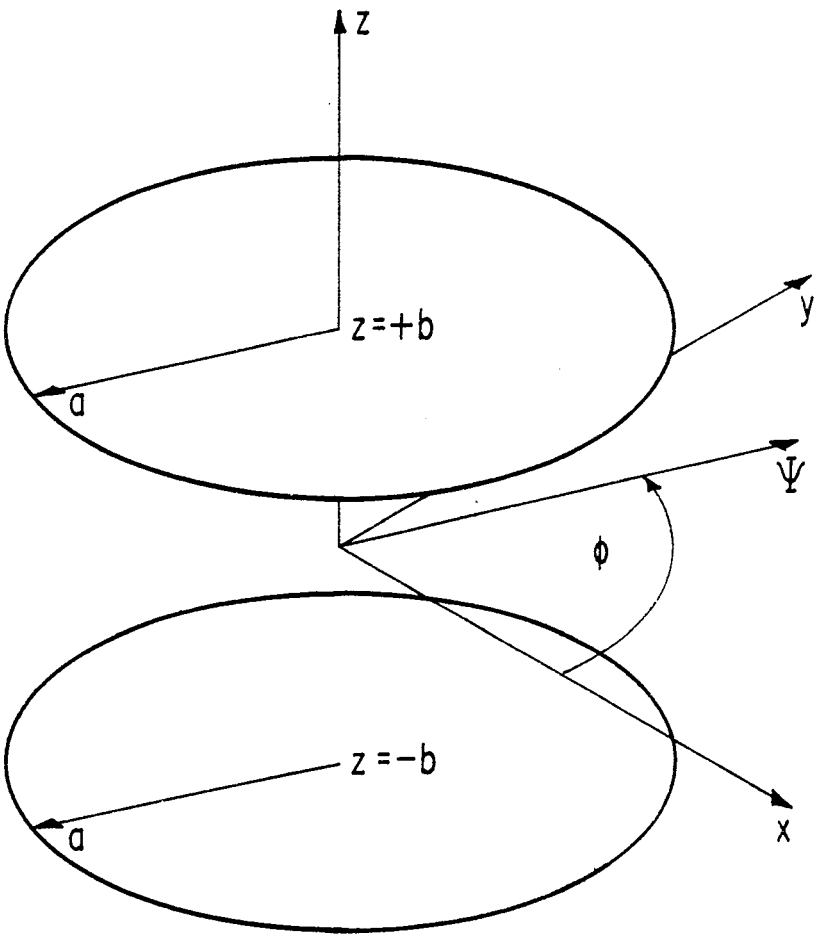


FIGURE 1. TWO EQUAL COAXIAL CIRCULAR DISKS WITH COORDINATES

This formula generally applies only for frequencies low enough that the corresponding wavelengths are much larger than the sensor dimensions.

For this particular type of sensor, however, the equivalent height can be used to somewhat higher frequencies provided the direction of wave incidence is appropriately restricted. Referring to figure 1 suppose we have an incident electromagnetic wave of the form

$$\vec{E}_{inc} = E_o \vec{e}_z e^{-j\vec{k}\cdot\vec{r}} \tag{3}$$

where $\omega$ is the radian frequency with $e^{j\omega t}$ suppressed, and where

$$\vec{r} \equiv x\vec{e}_x + y\vec{e}_y + z\vec{e}_z$$

$$k \equiv |\vec{k}| = \omega\sqrt{\mu\varepsilon}$$

$$\vec{k} \equiv k[\cos(\phi_o)\vec{e}_x + \sin(\phi_o)\vec{e}_y] \tag{4}$$

This is a plane wave with only a z component of the electric field, propagating parallel to the x, y plane in a direction given by $\phi = \phi_o$. The medium has permittivity $\varepsilon$ and permeability $\mu$; the conductivity is taken to be zero for our present discussion but the results can be directly extended to include an isotropic and homogeneous conductivity.

Note that an incident wave of the form in equation 3 is not perturbed by perfectly conducting sheets of zero thickness which are perpendicular to the electric field. Thus if we ignore the output connections on the sensor the parallel plate dipole in figure 1 will not distort this incident wave. Suppose for the moment that one were able to set up some apparatus which could respond to the line integral of $\vec{E}_{inc}$ between the two plates without loading the field. For symmetry take the line integral on the z axis giving

$$V_{oc} = -2bE_o \tag{5}$$

In such a case the equivalent height would apply to arbitrarily high frequencies with wavelengths much smaller than the sensor dimensions. Note that the radius of the plates (a) does not even enter into the problem.

Suppose now that one has some realistic but still high-impedance load connecting the two plates in the vicinity of the z axis. By high impedance we require that the load impedance be large compared to the impedance of the two plates for all $\omega$ greater than some $\omega_o$ of interest. Suppose, for example, that this load is some resistive rod or tube with total resistance R and with $RC = 1/\omega_o$ where C is the sensor capacitance (quasi static). If $a >> b$ and R is sufficiently large such that there is negligible load on the sensor for frequencies of interest, then the radius a of the sensor has little or no effect on the sensor response at these high frequencies. Of course, there will be some perturbation in the output signal taken at some small gap in the resistor due to the resistor dimensions and other resistor properties, but these are effects associated with the volume in the immediate vicinity of the resistor. If we assign some upper frequency response $\omega_1$ to the resistive output then as one makes a larger and larger the upper frequency response remains at $\omega_1$. On the other hand since C is roughly proportional to $a^2$ then $\omega_o$ continually decreases as a increases. Thus for the assumed type of incident wave with sufficiently large R and with $a >> b$ the upper frequency response is not limited by a but by the resistor characteristics.

As an illustration of this limitation of the high frequency response associated with an output resistor let $a \to \infty$ and consider the idealized problem illustrated in figure 2. Let the resistor be a cylindrical resistive sheet of radius $\Psi_o$ and surface resistance $R_s$. The resistance $R_1$ of this tube is then

$$R_1 = \frac{2b}{2\pi\Psi_o} R_s = \frac{b}{\pi\Psi_o} R_s \tag{6}$$

Since the geometry is assumed independent of $\phi$ we can set $\phi_o = 0$ for convenience so that the incident wave (equations 3 and 4) is propagating in the +x direction. In cylindrical coordinates $(\Psi, \phi, z)$ the incident electric field can be expanded as[2]

$$E_{z_{inc}} = E_o e^{-jk\Psi\cos(\phi)}$$

$$= E_o\left[J_o(k\Psi) + 2\sum_{n=1}^{\infty}(-j)^n J_n(k\Psi)\cos(n\phi)\right] \tag{7}$$

2. See AMS 55, Handbook of Mathematical Functions, National Bureau of Standards, 1964, for the expansions of $\cos[k\Psi\cos(\phi)]$ and $\sin[k\Psi\cos(\phi)]$.

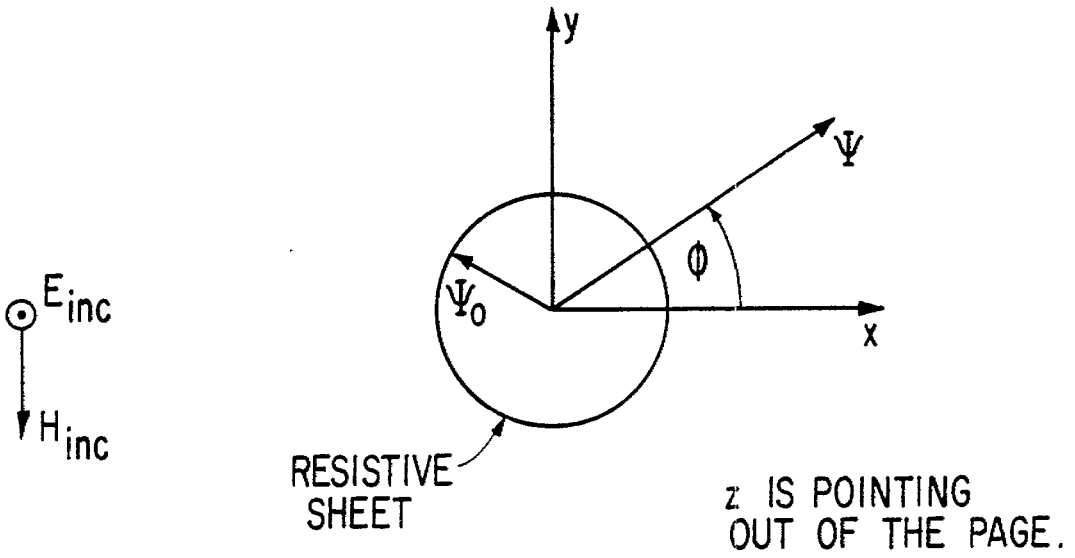


A. TOP VIEW

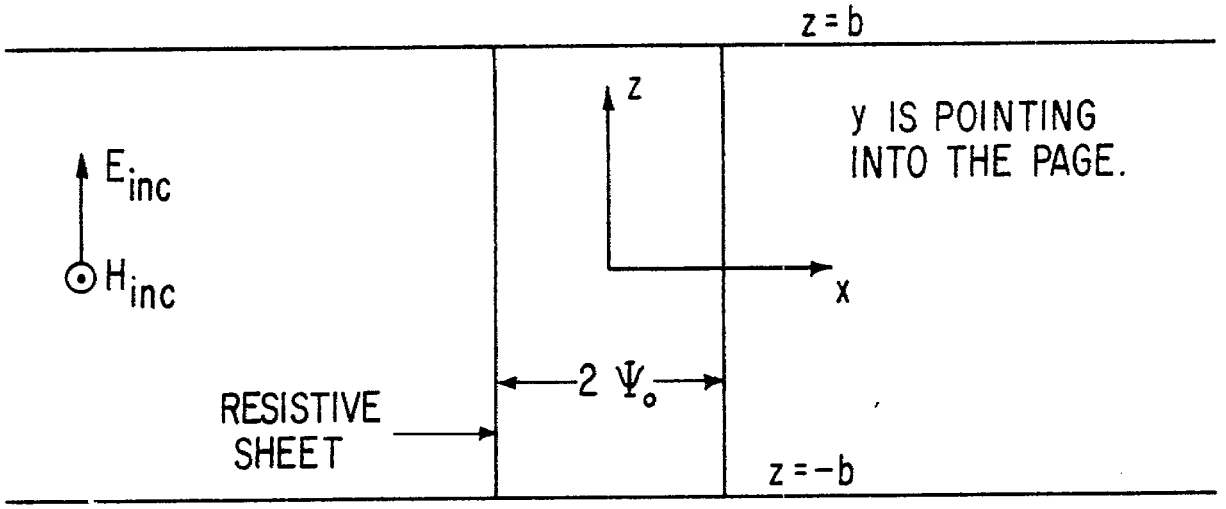


B. SIDE VIEW

FIGURE 2. IDEALIZED RESISTOR BETWEEN INFINITE PARALLEL PLATES

In cylindrical coordinates with only a z component of the electric field the field components can be expanded in the forms

$$E_z = E_o \sum_{n=o}^{\infty} \alpha_n C_n^{(\ell)}(k\Psi) \begin{Bmatrix} \cos(n\phi) \\ \sin(n\phi) \end{Bmatrix} \tag{8}$$

$$H_r = j \frac{E_o}{Z} \sum_{n=o}^{\infty} \alpha_n \frac{C_n^{(\ell)}(k\Psi)}{k\Psi} \begin{Bmatrix} -\sin(n\phi) \\ \cos(n\phi) \end{Bmatrix} \tag{9}$$

$$H_\phi = -j \frac{E_o}{Z} \sum_{n=o}^{\infty} \alpha_n C_n^{(\ell)'}(k\Psi) \begin{Bmatrix} \cos(n\phi) \\ \sin(n\phi) \end{Bmatrix} \tag{10}$$

where $C_n^{(\ell)}(k\Psi)$ denotes one of the cylindrical Bessel functions and a prime denotes the derivative with respect to the argument. The braces indicate a linear combination of the trigonometric functions inside the braces in a consistent manner for all three field components. The wave impedance is

$$Z \equiv \sqrt{\frac{\mu}{\varepsilon}} \tag{11}$$

The $\phi$ component of the incident magnetic field is then

$$H_{\phi_{inc}} = -j \frac{E_o}{Z} \left[ J_o'(k\Psi) + 2 \sum_{n=1}^{\infty} (-j)^n J_n'(k\Psi)\cos(n\phi) \right] \tag{12}$$

Using a subscript 1 we have two components of the fields for $\Psi < \Psi_o$ as

$$E_{z_1} = E_o \left[ a_o J_o(k\Psi) + 2 \sum_{n=1}^{\infty} (-j)^n a_n J_n(k\Psi)\cos(n\phi) \right] \tag{13}$$

$$H_{\phi_1} = -j \frac{E_o}{Z} \left[ a_o J_o'(k\Psi) + 2 \sum_{n=1}^{\infty} (-j)^n a_n J_n'(k\Psi)\cos(n\phi) \right] \tag{14}$$

Similarly, using a subscript 2 for the reflected wave for $\Psi > \Psi_o$ we have

$$E_{z_2} = E_o\left[b_o H_o^{(2)}(k\Psi) + 2\sum_{n=1}^{\infty}(-j)b_n H_n^{(2)}(k\Psi)\cos(n\phi)\right] \quad (15)$$

$$H_{\phi_2} = -j\frac{E_o}{Z}\left[b_o H_o^{(2)'}(k\Psi) + 2\sum_{n=1}^{\infty}(-j)^n b_n H_n^{(2)'}(k\Psi)\cos(n\phi)\right] \quad (16)$$

Now incorporate boundary conditions at $\Psi = \Psi_o$. Making $E_z$ continuous there gives

$$a_n J_n(k\Psi_o) = J_n(k\Psi_o) + b_n H_n^{(2)}(k\Psi_o) \quad (17)$$

which can be solved for $b_n$ to give

$$b_n = (a_n - 1)\frac{J_n(k\Psi_o)}{H_n^{(2)}(k\Psi_o)} \quad (18)$$

The surface current density at $\Psi = \Psi_o$ has only a z component given by

$$J_{s_z} = \left.\frac{E_{z_1}}{R_s}\right|_{\Psi=\Psi_o} = \frac{E_o}{R_s}\left[a_o J_o(k\Psi_o) + 2\sum_{n=1}^{\infty}(-j)^n J_n(k\Psi_o)\cos(n\phi)\right] \quad (19)$$

Another boundary condition relates the discontinuity of the magnetic field as

$$H_\phi\Big|_{\Psi=\Psi+} - H_\phi\Big|_{\Psi=\Psi-} = J_s \quad (20)$$

which gives

$$-j\frac{E_o}{Z}\left[J_n'(k\Psi_o) + b_n H_n^{(2)'}(k\Psi_o) - a_n J_n'(k\Psi_o)\right] = \frac{E_o}{R_s}a_n J_n(k\Psi_o) \quad (21)$$

Substituting for $b_n$ in equation 21 from equation 18 gives

$$(a_n-1)\left[-J_n'(k\Psi_o) + \frac{J_n(k\Psi_o)}{H_n^{(2)}(k\Psi_o)} H_n^{(2)'}(k\Psi_o)\right] = j\frac{Z}{R_s} a_n J_n(k\Psi_o) \quad (22)$$

Using a Wronskian relation for the Bessel functions gives

$$(a_n - 1)\left[\frac{-j2}{\pi k\Psi_o} \frac{1}{H_n^{(2)}(k\Psi_o)}\right] = j\frac{Z}{R_s} a_n J_n(k\Psi_o) \quad (23)$$

which can be solved for $a_n$ to give

$$a_n = \left[1 + \frac{Z}{R_s} \frac{\pi k\Psi_o}{2} J_n(k\Psi_o) H_n^{(2)}(k\Psi_o)\right]^{-1} \quad (24)$$

From equation 18 we have

$$b_n = -\frac{Z}{R_s} \frac{\pi k\Psi_o}{2} [J_n(k\Psi_o)]^2 \left[1 + \frac{Z}{R_s} \frac{\pi k\Psi_o}{2} J_n(k\Psi_o) H_n^{(2)}(k\Psi_o)\right]^{-1} \quad (25)$$

Now the current in this idealized resistor is just

$$I = \int_o^{2\pi} J_s \Psi_o d\phi = 2\pi\Psi_o \frac{E_o}{R_s} a_o J_o(k\Psi_o) \quad (26)$$

We define a reference or normalizing current as

$$I_o \equiv \frac{2bE_o}{R_l} = 2\pi\Psi_o \frac{E_o}{R_s} \quad (27)$$

In normalized form we can then write

$$\frac{I}{I_o} = a_o J_o(k\Psi_o) = J_o(k\Psi_o)\left[1 + \frac{Z}{R_s} \frac{\pi k\Psi_o}{2} J_o(k\Psi_o) H_o^{(2)}(k\Psi_o)\right]^{-1} \quad (28)$$

This is plotted in figure 3 for various values of $Z/R_s$. Note that for $Z/R_s < 1$ the upper frequency response is for $k\Psi_o$ of the order of one. This says that for sufficiently large $R_l$ the frequency response of the output current (I) is limited by $\Psi_o$, the

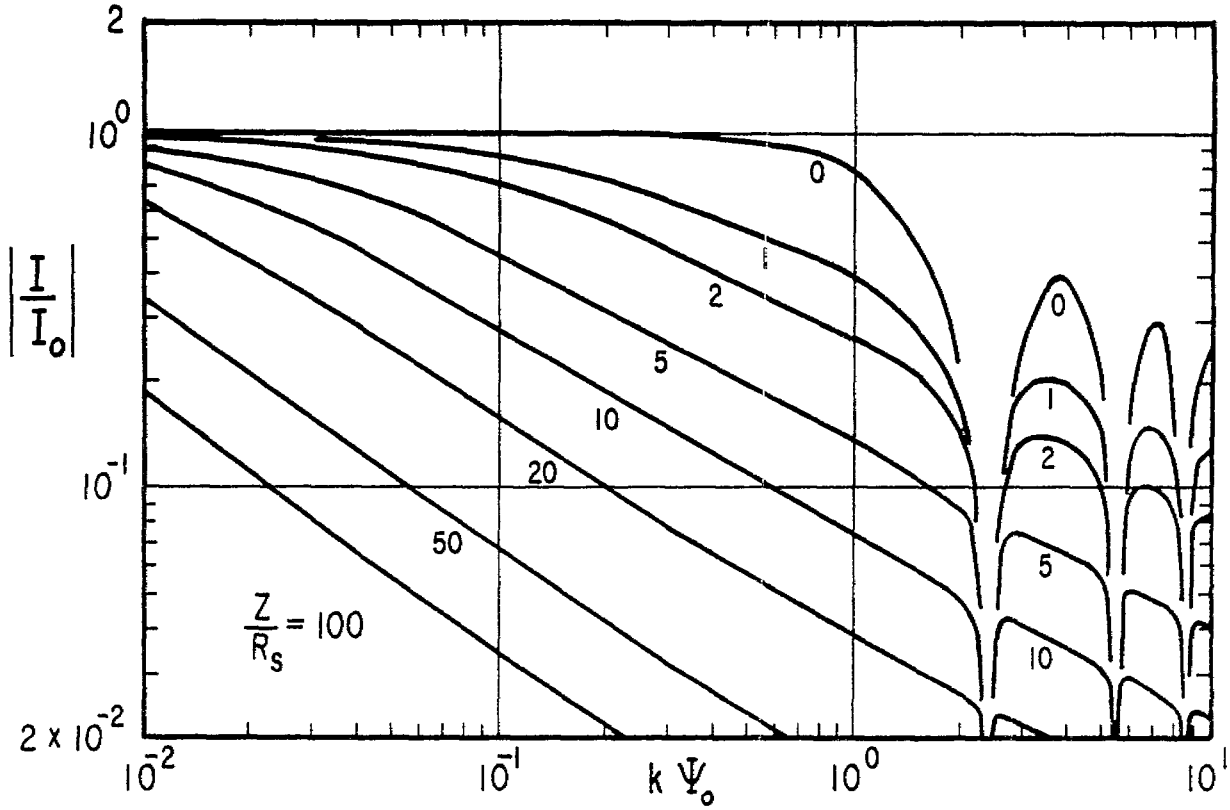


A. MAGNITUDE

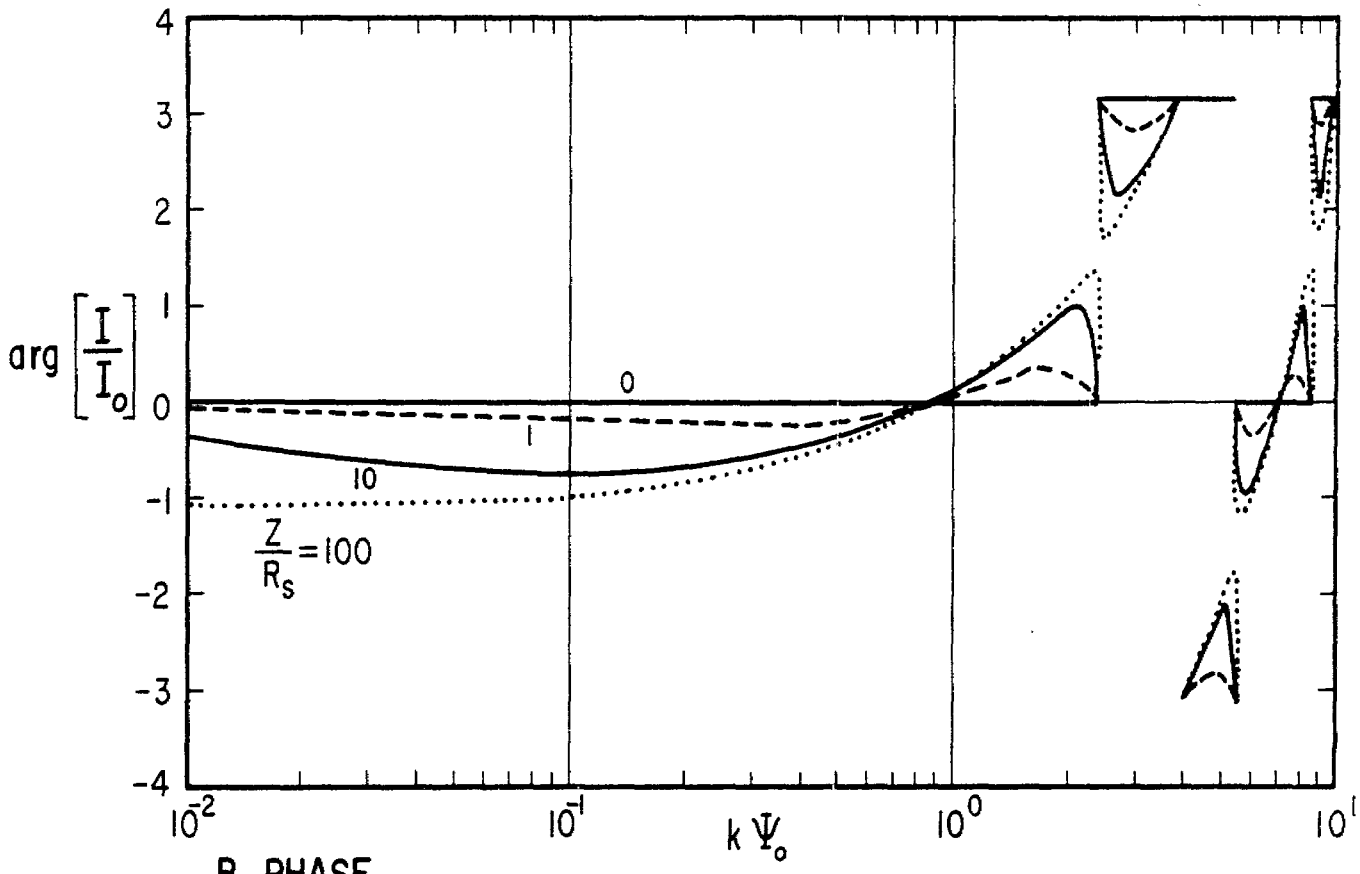


B. PHASE

FIGURE 3. CURRENT IN IDEALIZED RESISTOR

radius of the idealized resistor. Note that the magnitude of $I/I_o$ has zeros given by the zeros of $J_o(k\Psi_o)$; the first zero is at $k\Psi_o \simeq 2.405$. Also note that the wave reflected from the idealized resistor is small for $Z/R_s << 1$ as is evidenced by small $b_n$ in equation 25.

One of the problems in designing a parallel-plate dipole concerns the details of the output circuitry. If we consider a resistive output with large resistance then the frequency response of the sensor is basically limited by the local characteristics of the output circuitry. This, of course, applies to the case where the direction of wave incidence is parallel to the plates. In our idealized example considered above, the current in the output resistor (with large resistance) is limited in frequency response only by the diameter of the resistor. If one could sample or divert this current for recording purposes then the sensor should have rather high frequency response. For example one might put a load with small resistance $R_2$ in series with $R_1$ (such that $R_2 << R_1$) at one of the plates or at the $z = 0$ plane of symmetry. This would basically be a voltage divider network. $R_2$ might be the input impedance of a transmission line such as a coaxial or twinaxial cable.

While the response of the idealized resistor indicates a good high frequency response for the sensor there are problems yet to consider. For example, the output transmission line needs to be connected to the resistor in some manner, thereby altering the geometry. Perhaps other quantities besides I (as in equation 26), such as displacement current, will couple to the output transmission line. Other boundary value problems might be able to shed some light on this subject. Perhaps some such problems can be considered in future notes.

The parallel-plate dipole is then particularly suited for measuring electric fields when the direction of propagation of the incident wave is parallel to the plates. In equation 3 we have also taken the incident electric field to have a z component. However other polarizations can also be included provided appropriate symmetry is maintained in the sensor. Consider a circular parallel-plate dipole and choose the direction of propagation of the incident electric field as the +x direction; the incident electric field might also have a y component. Provided the sensor with its output conductors and circuit elements is symmetric with respect to the $z = 0$ plane (as illustrated), then the y component of the incident electric field produces no output signal. The incident wave can be considered as the linear superposition of two waves, one with a z component and one with a y component of the electric field, both propagating in the +x direction.

## III. Capacitance

It is rather straightforward to calculate the equivalent height of a parallel-plate dipole, provided the plate thickness is small compared to the plate spacing. However the capacitance of the sensor is more difficult to obtain. The simple formula which approximates the capacitance C as $\varepsilon\pi a^2/(2b)$ is not very accurate unless a/b is extremely large. The fringe fields (the fields not between the two plates when charge is transferred between the plates) make a significant contribution to the capacitance.

First define a normalized capacitance

$$\gamma \equiv \frac{C}{\varepsilon a} \tag{29}$$

where C is the sensor capacitance. Define a normalized variable

$$\lambda \equiv \frac{2b}{a} \tag{30}$$

The capacitance can be obtained from a function $f(\zeta)$ which satisfies an integral equation obtained by Love,[3] specifically

$$f(\zeta) = 1 + \frac{1}{\pi}\int_{-1}^{1} \frac{\lambda}{\lambda^2 + (\zeta - \zeta')^2} f(\zeta')d\zeta' \tag{31}$$

If the upper plate at z = b has potential $V_o$ and charge Q, and if the lower plate at z = -b has potential $-V_o$ and charge -Q the capacitance is just

$$C \equiv \frac{Q}{2V_o} \tag{32}$$

From Love the charge on the upper plate (in MKSA units) is just

$$Q = 4V_o\varepsilon a\int_{-1}^{1} f(\zeta)d\zeta \tag{33}$$

3. E. R. Love, The Electrostatic Field of Two Equal Circular Coaxial Conducting Disks, Quart. J. Mech. and Applied Math., 2, 1949, pp. 428-451.

giving a capacitance

$$C = 2\varepsilon a \int_{-1}^{1} f(\zeta)d\zeta \tag{34}$$

which in normalized form is

$$\gamma = 2\int_{-1}^{1} f(\zeta)d\zeta \tag{35}$$

The potential $\Phi$ at any point ($\Psi$, $\phi$, z) is given by

$$\Phi = \frac{V_o}{\pi}\int_{-1}^{1}\left\{\left[\left(\frac{\Psi}{a}\right)^2 + \left(\frac{z-b}{a} + j\zeta\right)^2\right]^{-1/2} - \left[\left(\frac{\Psi}{a}\right)^2 + \left(\frac{z+b}{a} + j\zeta\right)^2\right]^{-1/2}\right\} f(\zeta)d\zeta \tag{36}$$

For details of the derivations the reader is referred to Love's paper. Basically $\Phi$ as in equation 36 is shown to satisfy the Laplace equation away from both plates; $\Phi$ becomes $\pm V_o$ on the two plates provided $f(\zeta)$ satisfies equation 31. The charge density on one of the plates can be found by multiplying $\varepsilon$ times the discontinuity in $-\partial\Phi/\partial z$ at the plate.

In appendix A we consider the numerical solution of equation 31. In figure 4 the normalized capacitance is plotted as a function of $\lambda$. This is also tabulated in table 1 at the end of the note. For comparison to the short table in Cooke[4] we have

$$A_o \equiv \frac{1}{2}\int_{-1}^{1} f(\zeta)d\zeta = \frac{\gamma}{4} \tag{37}$$

As an aid in calculating $\gamma$ consider asymptotic forms for small and large $\lambda$. For small $\lambda$ so that a >> b (a case of interest

4. J. C. Cooke, The Coaxial Circular Disk Problem, Z. angew. Math. Mech. Bd. 38 Nr. 9/10, 1958, pp. 349-356.

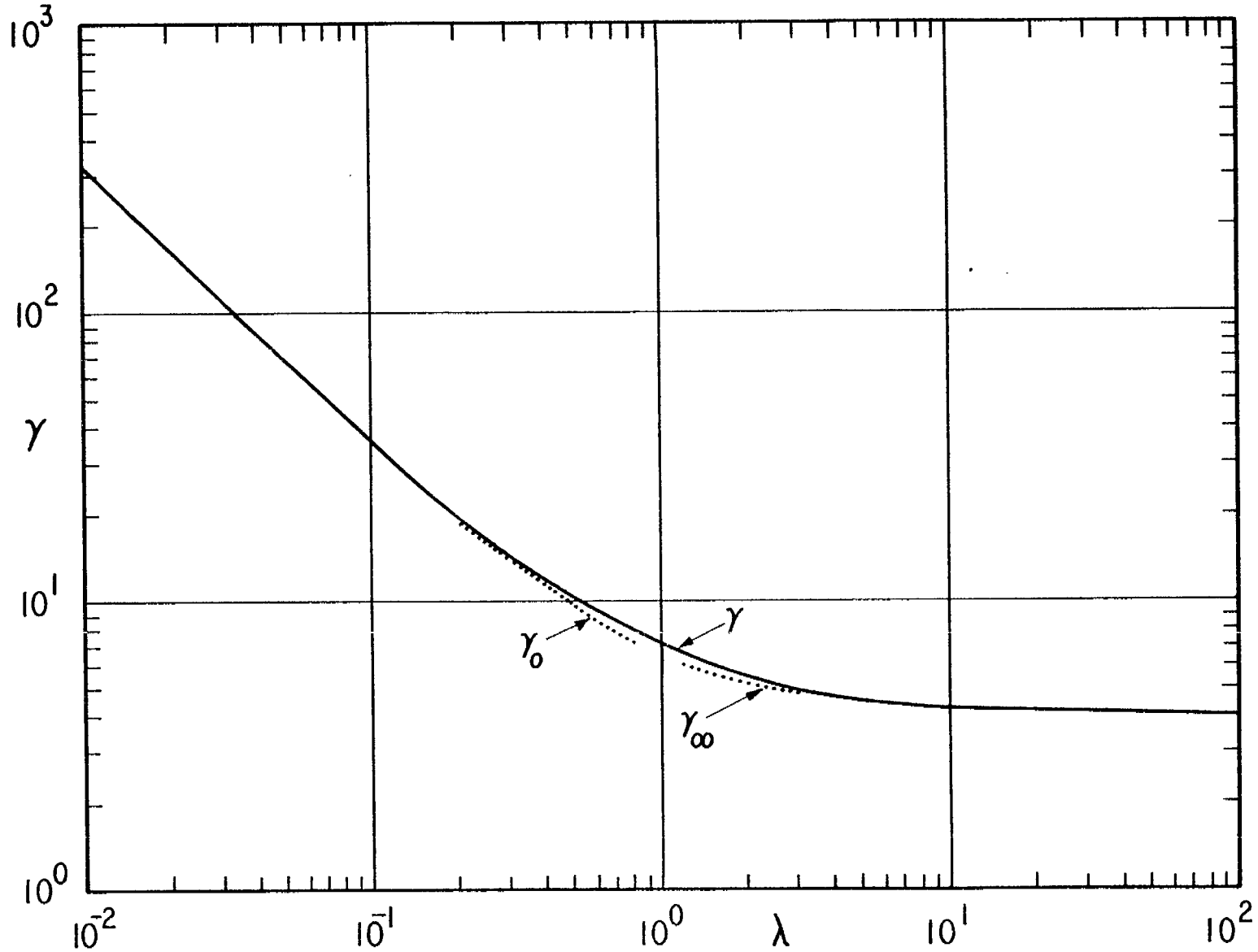


FIGURE 4. NORMALIZED CAPACITANCE

for a sensor) the asymptotic form for $\gamma$ was found by Hutson[5] who showed that as $\lambda \to 0$

$$\gamma = \frac{\pi}{\lambda} + \ln\left(\frac{16\pi}{\lambda}\right) - 1 + o(1) \tag{38}$$

For convenience we then define

$$\gamma_o \equiv \frac{\pi}{\lambda} + \ln\left(\frac{16\pi}{\lambda}\right) - 1 \tag{39}$$

so that $\gamma - \gamma_o \to 0$ as $\lambda \to 0$. Writing out equation 39 for the capacitance we have as $\lambda \to 0$

$$C = \varepsilon a\gamma = \varepsilon\left\{\frac{\pi a^2}{2b} + a\left[\ln\left(\frac{8\pi a}{b}\right) - 1\right]\right\} + o(1) \tag{40}$$

The first term in the braces corresponds to the simple area over spacing formula often used; the remaining terms give the error when such a simple formula is used.

The asymptotic form in equations 38 through 40 corresponds to Kirchoff's result for small $\lambda$. Let the plate thickness be assumed for the moment to be non zero and call it w (the same for both plates). Let 2b be the spacing between adjacent faces of the two plates. Also let the edges be square. Then we quote Kirchoff's result for the capacitance C' for small $\lambda$ as[6]

$$C' \simeq \varepsilon\left\{\frac{\pi a^2}{2b} + a\left\{\ln\left[\frac{8\pi a}{b}\left(1 + \frac{w}{2b}\right)\right] - 1 + \frac{2\pi w}{b}\ln\left[1 + \frac{2b}{w}\right]\right\}\right\} \tag{41}$$

Then we can attribute an increase in capacitance $\Delta C$ due to the finite plate thickness with square edges as

$$\Delta C \equiv C' - C \simeq \varepsilon a\left\{\ln\left[1 + \frac{w}{2b}\right] + \frac{2\pi w}{b}\ln\left[1 + \frac{2b}{w}\right]\right\} \tag{42}$$

The corresponding increase in $\gamma$ is

5. V. Hutson, The Circular Plate Condenser at Small Separations, Proc. Camb. Phil. Soc., 59, 1963, pp. 211-224.

6. American Institute of Physics Handbook, 2nd ed., McGraw-Hill, 1963, section 5, p. 14.

$$\Delta\gamma \equiv \frac{\Delta C}{\varepsilon a} \simeq \ln\left[1 + \frac{w}{2b}\right] + \frac{2\pi w}{b} \ln\left[1 + \frac{2b}{w}\right] \tag{43}$$

This can be used as an approximation to the increase in sensor capacitance due to finite plate thickness with square edges. However, to the author's knowledge this result has not been rigorously established in the sense that $\gamma_o$ has been established by Hutson as the asymptotic form for small $\lambda$ with $w = 0$.

Next consider the case of large $\lambda$ for which $a << b$. Let the disks have zero thickness. As $\lambda \to \infty$ the problem becomes one of considering the capacitance of two isolated disks of radius a. The capacitance tends to 1/2 the capacitance of a single isolated disk. Then using the result from Smythe[7] the capacitance for $\lambda \to \infty$ has the form

$$C \to \frac{1}{2} (8\varepsilon a) = 4\varepsilon a \tag{44}$$

so that as $\lambda \to \infty$

$$\gamma \to 4 \tag{45}$$

Now, as shown by Love (reference 3), the solution of equation 31 can be written as the Neumann series

$$f(\zeta) = 1 + \sum_{n=1}^{\infty} \left\{ \int_{-1}^{1} K_n(\zeta, \zeta')d\zeta' \right\} \tag{46}$$

where $K_1$ is the kernal of the integral equation defined by

$$K_1(\zeta, \zeta') \equiv \frac{1}{\pi} \frac{\lambda}{\lambda^2 + (\zeta - \zeta')^2} \tag{47}$$

and where the remaining $K_n$ are the iterated kernals defined by

$$K_n(\zeta, \zeta') \equiv \int_{-1}^{1} K_{n-1}(\zeta, \zeta'')K_1(\zeta'', \zeta')d\zeta''$$

$$\text{for } n = 2, 3, \ldots \tag{48}$$

7. W. R. Smythe, Static and Dynamic Electricity, 2nd ed., McGraw-Hill, 1950, p. 114.

Define a truncated Neumann series as

$$f_M(\zeta) \equiv 1 + \sum_{n=1}^{M} \left\{ \int_{-1}^{1} K_n(\zeta, \zeta')d\zeta' \right\} \quad \text{for } M = 0, 1, 2, \ldots \tag{49}$$

(For $M = 0$ we have $f_0(\zeta) \equiv 1$.) Love shows that

$$f(\zeta) = f_M(\zeta) + R_M(\zeta) \tag{50}$$

where the remainder $R_M(\zeta)$ is of the order of $\left[\frac{2}{\pi} \arctan\left(\frac{1}{\lambda}\right)\right]^M$ so that (with $\lambda > 0$) as $N \to \infty$ the remainder goes to zero.

Now consider the asymptotic form of $\gamma$ for large $\lambda$. For convenience define

$$\nu \equiv \frac{1}{\lambda} \tag{51}$$

so that we are concerned with asymptotic forms as $\nu \to 0$. Consider the first few terms of the Neumann series. We have as $\nu \to 0$

$$f_1(\zeta) = 1 + \frac{1}{\pi} \int_{-1}^{1} \frac{\nu}{1 + \nu^2(\zeta - \zeta')^2} d\zeta'$$

$$= 1 + \frac{1}{\pi} \int_{-\nu-\nu\zeta}^{\nu-\nu\zeta} [1 + \alpha^2]^{-1} d\alpha$$

$$= 1 + \frac{1}{\pi} [\arctan(\nu - \nu\zeta) + \arctan(\nu + \nu\zeta)]$$

$$= 1 + \frac{2\nu}{\pi} + O(\nu^3) \tag{52}$$

where we have used the substitution $\alpha \equiv \nu\zeta' - \nu\zeta$. Now as $\nu \to 0$

$$K_1(\zeta, \zeta') = O(\nu)$$

$$K_2(\zeta, \zeta') = O(\nu^2)$$

$$K_n(\zeta, \zeta') = O(\nu^n) \tag{53}$$

From this we have

$$f_2(\zeta) = f_1(\zeta) + O(\nu^2) \tag{54}$$

From Love's result

$$f(\zeta) - f_2(\zeta) = R_2(\zeta) = O(\nu^2) \tag{55}$$

Thus we have for $\nu \to 0$

$$f(\zeta) = 1 + \frac{2\nu}{\pi} + O(\nu^2) \tag{56}$$

and then for $\gamma$ as $\nu \to 0$ we have

$$\gamma = 2 \int_{-1}^{1} f(\zeta) d\zeta = 4\left[1 + \frac{2\nu}{\pi}\right] + O(\nu^2) \tag{57}$$

Based on this result define

$$\gamma_\infty \equiv 4\left[1 + \frac{2\nu}{\pi}\right] = 4\left[1 + \frac{2}{\pi\lambda}\right] \tag{58}$$

so that $\gamma - \gamma_\infty = O(\lambda^{-2})$ as $\lambda \to \infty$.

Having the capacitance and equivalent height we can calculate the equivalent volume as[8,9]

$$V_{eq} = \frac{C}{\varepsilon} \vec{h}_{eq} \cdot \vec{h}_{eq} = 4b^2 a\gamma \tag{59}$$

8. Capt Carl E. Baum, Sensor and Simulation Note 38, Parameters for Some Electrically-Small Electromagnetic Sensors, March 1967.

9. Capt Carl E. Baum, Sensor and Simulation Note 74, Parameters for Electrically-Small Loops and Dipoles Expressed in Terms of Current and Charge Distributions, January 1969.

Define a geometric volume as the volume of the smallest sphere which encloses the sensor. This sphere has a radius

$$r_s = [a^2 + b^2]^{1/2} = a\left[1 + \left(\frac{\lambda}{2}\right)^2\right]^{1/2} \tag{60}$$

The reference geometric volume is then

$$V_g = \frac{4}{3}\pi r_s^3 \tag{61}$$

and the figure of merit based on this spherical volume is then

$$\eta_s \equiv \frac{V_{eq}}{V_g} = \frac{3}{4\pi}\,\frac{\lambda^2\gamma}{\left[1 + \left(\frac{\lambda}{2}\right)^2\right]^{3/2}} \tag{62}$$

This figure of merit is plotted in figure 5 and also tabulated in table 1.

Referring to figure 5 the maximum $\eta_s$ is about 1.9; the corresponding $\lambda$ is about 2.3. However for the present type of parallel plate dipole one would typically design it with a small $\lambda$ and use a resistive divider on the output. Due to the presence of this additional resistor in series with the sensor output the figure of merit concept does not have the same direct application as discussed in reference 8.

## IV. Low-Frequency Electric Field Distortion Due to a Spherical Dielectric Shell

For mechanical protection of the sensor one might wish to enclose the sensor in a dielectric shell. Also one might wish to enclose some material (in the immediate vicinity of the sensor) which has a higher dielectric strength than the surrounding medium; this higher-dielectric-strength material is assumed to have the same permittivity and permeability as the surrounding medium. However, the dielectric shell may have a permittivity which differs from the permittivity of the surrounding medium. This shell may then distort the incident electric field, thereby affecting the sensor response. Of course, if the shell is sufficiently thin we would normally expect the distortion to be small.

In this section we assume that there is a spherical dielectric shell of permittivity $\varepsilon_2$, inner radius $r_1$, and outer radius

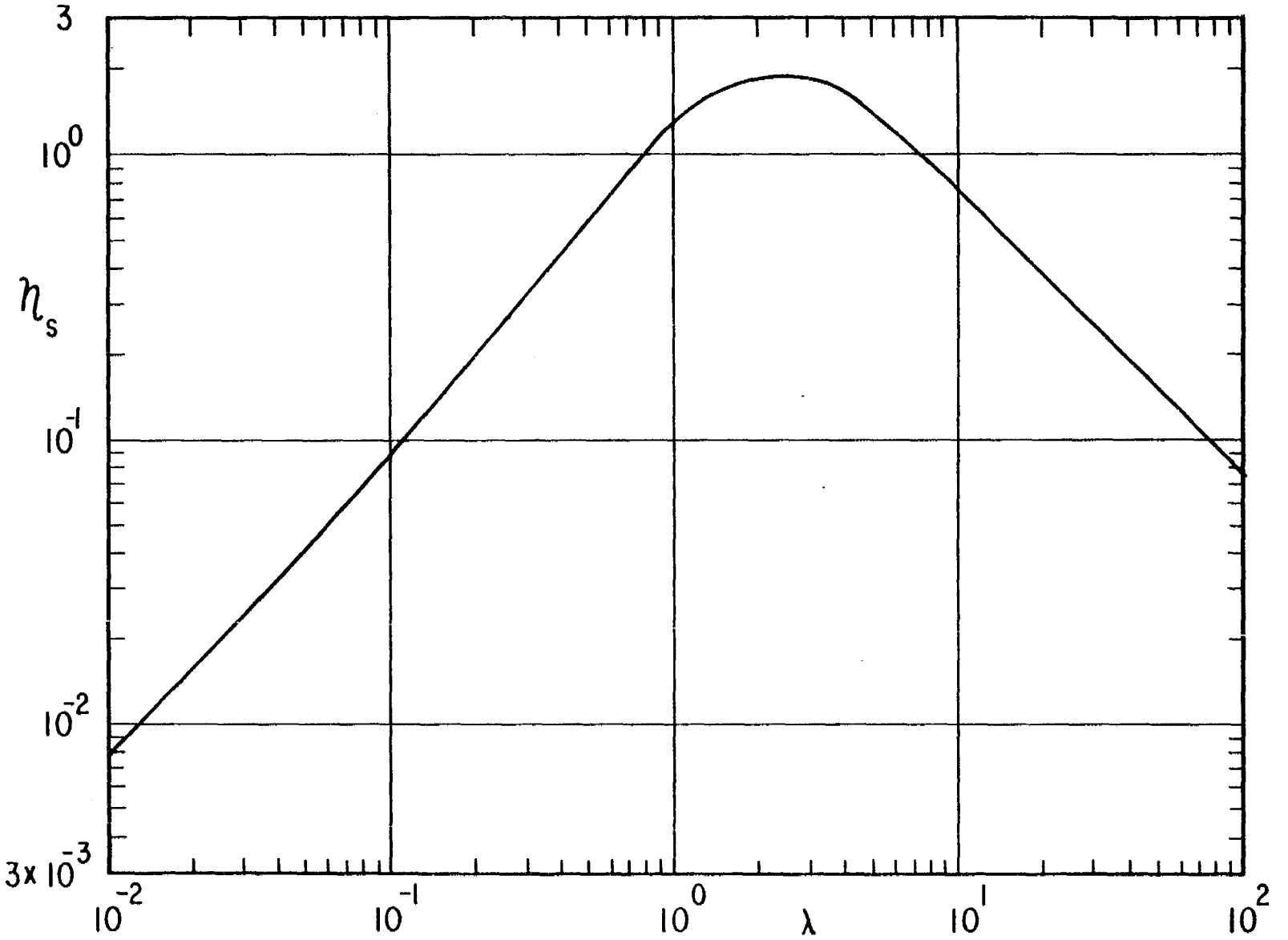


FIGURE 5. FIGURE OF MERIT

$r_2$ as illustrated in figure 6. For convenience define

$$d \equiv r_2 - r_1$$

$$D \equiv \frac{d}{r_2} \tag{63}$$

$$\varepsilon_r \equiv \frac{\varepsilon_2}{\varepsilon_1}$$

where $\varepsilon_1$ is the permittivity of the media both inside and outside the shell. All media have the same permeability $\mu$ and all have zero conductivity. Furthermore we only consider frequencies with wavelengths much larger than $2r_2$ so that we can use a quasi static calculation of the electric field distortion.

Assume a uniform incident static electric field of the form

$$\vec{E}_{inc} \equiv E_o \vec{e}_z = E_o \vec{e}_r \cos(\theta) - E_o \vec{e}_\theta \sin(\theta) \tag{64}$$

and a corresponding incident potential of the form

$$\Phi_{inc} = -E_o z = -E_o r \cos(\theta) = -E_o r P_1(\cos(\theta)) \tag{65}$$

where $P_1$ is one of the Legendre functions of the first kind. Assuming for the present discussion that no sensor is present we have a spherically symmetric boundary value problem. Expanding the solution of the Laplace equation in spherical ($r$, $\theta$, $\phi$) coordinates as appropriate to each region of space we have for $r \leq r_1$

$$\Phi_1 = -E_o \cos(\theta) a_1 r \tag{66}$$

for $r_1 \leq r \leq r_2$

$$\Phi_2 = -E_o \cos(\theta) \left[ a_2 r + \frac{b_2}{r^2} \right] \tag{67}$$

and for $r_2 \leq r$

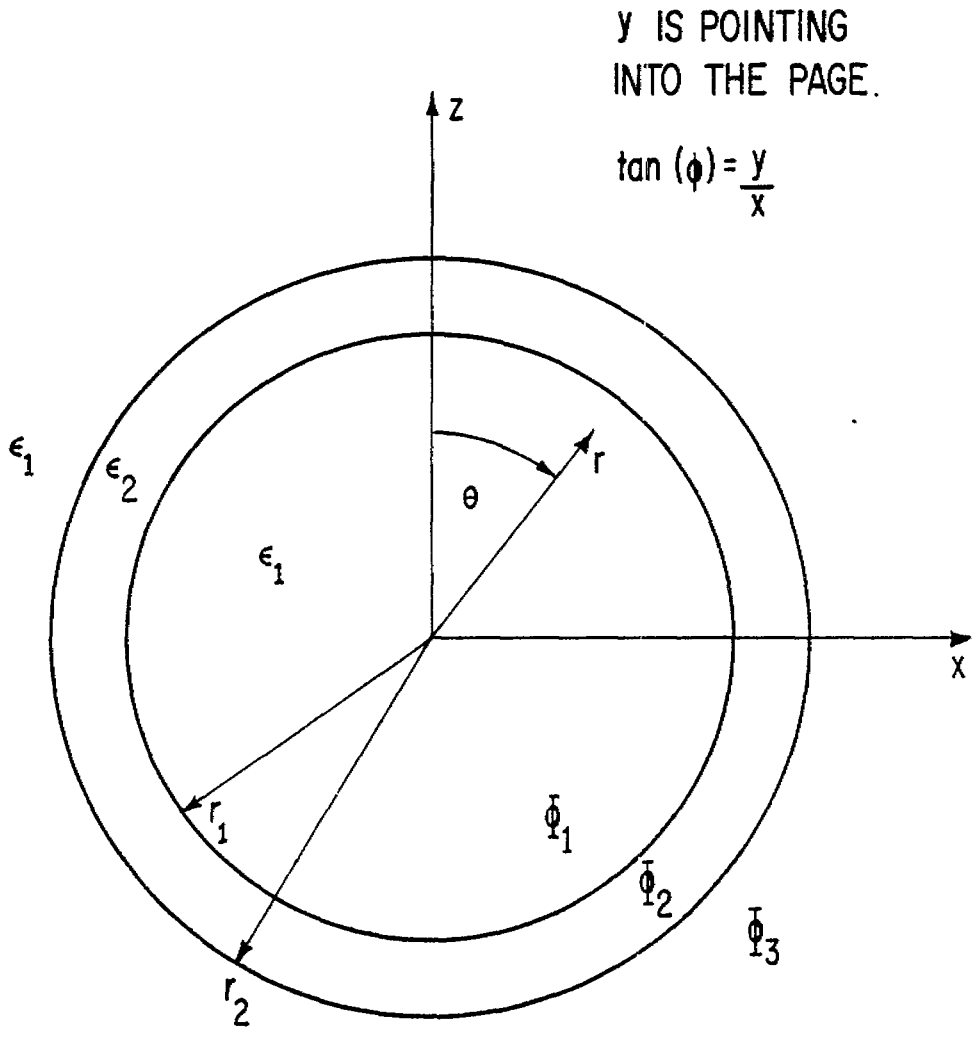


FIGURE 6. SPHERICAL DIELECTRIC SHELL

$$\Phi_3 = \Phi_{inc} - E_o \cos(\theta) \frac{b_3}{r^2} = -E_o \cos(\theta)\left[r + \frac{b_3}{r^2}\right] \tag{68}$$

Consider next the boundary conditions at the two interfaces. At each interface $\Phi$ and $-\varepsilon(\partial\Phi/\partial r)$ (the normal component of the displacement vector) must be continuous. Then by setting $r = r_1$ we obtain

$$\begin{aligned} a_1 &= a_2 + \frac{b_2}{r_1^3} \\ a_1 &= \varepsilon_r\left[a_2 - \frac{2b_2}{r_1^3}\right] \end{aligned} \tag{69}$$

which gives

$$(1 - \varepsilon_r)a_2 + (1 + 2\varepsilon_r)\frac{b_2}{r_1^3} = 0 \tag{70}$$

By setting $r = r_2$ we obtain

$$\begin{aligned} a_2 + \frac{b_2}{r_2^3} &= 1 + \frac{b_3}{r_2^3} \\ \varepsilon_r\left[a_2 - 2\frac{b_2}{r_2^3}\right] &= 1 - 2\frac{b_3}{r_2^3} \end{aligned} \tag{71}$$

which gives

$$(2 + \varepsilon_r)a_2 + 2(1 - \varepsilon_r)\frac{b_2}{r_2^3} = 3 \tag{72}$$

Combining equations 70 and 72 we have

$$\left[\frac{1}{r_1^3}(1+2\varepsilon_r)(2+\varepsilon_r) - \frac{2}{r_2^3}(1-\varepsilon_r)^2\right]a_2 = \frac{3}{r_1^3}(1+2\varepsilon_r)$$

$$\left[\frac{1}{r_1^3}(1+2\varepsilon_r)(2+\varepsilon_r) - \frac{2}{r_2^3}(1-\varepsilon_r)^2\right]b_2 = -3(1-\varepsilon_r) \tag{73}$$

Then from the first of equations 69 we have

$$a_1 = \frac{9\varepsilon_r}{(1+2\varepsilon_r)(2+\varepsilon_r) - 2\left(\frac{r_1}{r_2}\right)^3(1-\varepsilon_r)^2} \tag{74}$$

The potential inside the spherical shell is then

$$\Phi_1 = -E_o\cos(\theta)a_1 r = -E_o a_1 z \tag{75}$$

The corresponding electric field is given by

$$\vec{E}_1 = -\nabla\Phi_1 = E_o a_1 \vec{e}_z \tag{76}$$

The electric field inside the shell is then a uniform field in the same direction as the uniform incident field as in equation 64. Note that conducting sheets of zero thickness can be placed perpendicular to the z axis without distorting the field. The present results can then be used to correct the open circuit voltage (and thereby the equivalent height) due to the presence of the spherical dielectric shell.

Consider the field reduction factor $a_1$. For small D we have

$$\left(\frac{r_1}{r_2}\right)^3 = (1-D)^3 \simeq 1 - 3D \tag{77}$$

Then for $D << 1$ we can expand $a_1$ as

$$a_1 \simeq \frac{9\varepsilon_r}{9\varepsilon_r + 6D(1-\varepsilon_r)^2}$$

$$= [1 + \Lambda]^{-1}$$

$$\simeq 1 - \Lambda \tag{78}$$

where we define

$$\Lambda \equiv \frac{2D}{3\varepsilon_r} (1 - \varepsilon_r)^2 \tag{79}$$

$\Lambda$ is a measure of the electric field distortion introduced by the presence of the dielectric shell. As one would expect this distortion is small for small D and for small $\varepsilon_r - 1$.

## V. Summary

A parallel-plate dipole has certain desirable features, such as an accurately calculable equivalent height. Furthermore if the direction of wave incidence is parallel to the plates the upper frequency response can be very high, limited by the details of the output circuitry rather than the size of the plates. For very thin coaxial circular plates the capacitance can also be calculated by a numerical solution of a particular integral equation.

For various reasons the dipole may be enclosed in a dielectric shell. A thin spherical shell with a not-too-large dielectric constant distorts the incident electric field very little. One would also expect small electric field distortion from other similar types of thin shells for enclosing the sensor.

We would like to thank A2C Richard T. Clark and Mr. Larry D. Giorgi for the numerical calculations and graphs.

## Appendix A: Numerical Calculation of Normalized Capacitance

In order to calculate the normalized capacitance $\gamma$ we numerically solve equation 31, the integral equation which we repeat here as

$$f(\zeta) = 1 + \frac{1}{\pi} \int_{-1}^{1} \frac{\lambda}{\lambda^2 + (\zeta - \zeta')^2} f(\zeta')d\zeta' \tag{A1}$$

The normalized capacitance from equation 35 is

$$\gamma = 2 \int_{-1}^{1} f(\zeta)d\zeta \tag{A2}$$

The method of numerical solution is that discussed by Fox and Goodwin.[1a]

We begin by taking advantage of the special form of $f(\zeta)$, namely that it is even in $\zeta$ (shown in reference 3). In equation A1 we can then replace $\zeta'$ by $-\zeta'$, add this new form of equation A1 to the original form, and then divide by 2 to give

$$f(\zeta) = 1 + \frac{1}{2\pi} \int_{-1}^{1} \left[ \frac{\lambda}{\lambda^2+(\zeta-\zeta')^2} + \frac{\lambda}{\lambda^2+(\zeta+\zeta')^2} \right] f(\zeta')d\zeta' \tag{A3}$$

The integrand is now even in $\zeta'$ which allows us to write

$$f(\zeta) = 1 + \frac{1}{\pi} \int_{o}^{1} \left[ \frac{\lambda}{\lambda^2+(\zeta-\zeta')^2} + \frac{\lambda}{\lambda^2+(\zeta+\zeta')^2} \right] f(\zeta')d\zeta' \tag{A4}$$

The normalized capacitance can also be expressed as

$$\gamma = 4 \int_{o}^{1} f(\zeta)d\zeta \tag{A5}$$

---

1a. L. Fox and E. T. Goodwin, The Numerical Solution of Non-Singular Linear Integral Equations, Phil. Trans. Roy. Soc. of London, 245A, 1953, pp. 501-534.

For our numerical solution the integrals are approximated as sums over a finite set of points. The Gregory integration formula is given by[2a]

$$\int_{\zeta_o}^{\zeta_1} p(\zeta)d\zeta = h\left[\frac{p_1+p_N}{2} + \sum_{k=2}^{N-1} p_k\right] - \frac{h}{12}\left(\nabla p_N - \Delta p_1\right)$$

$$- \frac{h}{24}\left(\nabla^2 p_N + \Delta^2 p_1\right) - \frac{19h}{720}\left(\nabla^3 p_N - \Delta^3 p_1\right)$$

$$- \frac{3h}{160}\left(\nabla^4 p_N + \Delta^4 p_1\right) - \frac{863h}{60480}\left(\nabla^5 p_N - \Delta^5 p_1\right) - \ldots \quad \text{(A6)}$$

This formula is used for the present numerical results with differences only up to the third order retained. For this formula the interval $\zeta_o$ to $\zeta$ is divided by N evenly spaced points, $p_1$ to $p_N$ (including the end points). The interval size is

$$h \equiv \frac{\zeta_o - \zeta_1}{N - 1} \quad \text{(A7)}$$

The forward differences are defined inductively by

$$\Delta^1 p_k \equiv \Delta p_k \equiv p_{k+1} - p_k$$

$$\Delta^n p_k \equiv \Delta^{n-1} p_{k+1} - \Delta^{n-1} p_k \qquad \text{for } n = 2, 3, 4, \ldots \quad \text{(A8)}$$

The backward differences are similarly defined as

$$\nabla^1 p_k \equiv \nabla p_k \equiv p_k - p_{k-1}$$

$$\nabla^n p_k \equiv \nabla^{n-1} p_k - \nabla^{n-1} p_{k-1} \qquad \text{for } n = 2, 3, 4, \ldots \quad \text{(A9)}$$

For the numerical solution of equation A4 first define

2a. F. B. Hildebrand, Introduction to Numerical Analysis, McGraw-Hill, 1956, p. 155.

$$\zeta_k \equiv \frac{k-1}{N-1} \qquad k = 1, 2, \ldots, N \tag{A10}$$

so that the interval 0 to 1 is divided into N evenly spaced points (including the endpoints). Then define

$$f_j \equiv f(\zeta_j) \qquad \text{for } j = 1, 2, \ldots, N \tag{A11}$$

$$g_{jk} \equiv \frac{h}{\pi}\left[\frac{\lambda}{\lambda^2+(\zeta_j-\zeta_k)^2} + \frac{\lambda}{\lambda^2+(\zeta_j+\zeta_k)^2}\right] \text{ for } j,k = 1,2,\ldots,N \tag{A12}$$

$$g'_{jk} \equiv \begin{cases} \frac{1}{2}\, g_{jk} & \text{for } k = 1, N \\ g_{jk} & \text{for } k = 2, 3, \ldots, N-1 \end{cases} \qquad \text{for } j = 1, 2, \ldots, N \tag{A13}$$

where for these and succeeding equations we have

$$h \equiv \frac{1}{N-1} \tag{A14}$$

Equation A4 can now be written for the $f_j$ as

$$f_j = 1 + \left[\sum_{k=1}^{N} g'_{jk} f_k\right] + \Delta_j \tag{A15}$$

Using the $g'_{jk}$ this equation has written the integral in equation A4 as a trapezoidal sum plus a correction term $\Delta_j$. From the Gregory integration formula this is just

$$\Delta_j = -\frac{1}{12}\left[\nabla(g_{jN}f_N)-\Delta(g_{j1}f_1)\right] - \frac{1}{24}\left[\nabla^2(g_{jN}f_N)+\Delta^2(g_{j1}f_1)\right]$$

$$- \frac{19}{720}\left[\nabla^3(g_{jN}f_N)-\Delta^3(g_{j1}f_1)\right] - \ldots \tag{A16}$$

where differences up to the third order have been kept.

Define $\vec{f}$ and $\vec{\Delta}$ as N component vectors with components $f_j$ and $\Delta_j$ respectively. We can use the $g_{jk}$ and $g'_{jk}$ to form N x N matrices $(g_{jk})$ and $(g'_{jk})$. Define $\vec{1}$ as the N component vector with all N components equal to 1. The N x N identity matrix is $(\delta_{jk})$ where $\delta_{jk}$ is the Kronecker delta function defined by

$$\delta_{jk} \equiv \begin{cases} 1 \text{ for } j = k \\ 0 \text{ for } j \neq k \end{cases} \tag{A17}$$

Equation A15 can be rewritten using vectors and matrices as

$$\vec{f} = \vec{1} + (g'_{jk}) \cdot \vec{f} + \vec{\Delta}(g_{jk}f_k) \tag{A18}$$

or

$$[(\delta_{jk}) - (g'_{jk})] \cdot \vec{f} = \vec{1} + \vec{\Delta}(g_{jk}f_k) \tag{A19}$$

Note that $\vec{\Delta}$ is a correction vector expressing the Gregory correction terms which correct the trapezoidal integration formula. $\vec{\Delta}$ can be considered a linear vector finite difference operator, operating in this case on the matrix $(g_{jk}f_k)$. For purposes of the present calculations we only use the differences in equation A16 up to third order. Thus only k = 1, 2, 3, 4 and k = N - 3, N - 2, N - 1, N are used from $(g_{jk}f_k)$ in forming the forward and backward differences. Having defined $\vec{\Delta}$ as a vector difference operator we can use it to operate on various N x N matrices.

For the solution of our numerical problem, following reference 1a we do an iterative solution. Having specified an N we can calculate a matrix inverse which we define by

$$B \equiv A^{-1} \tag{A20}$$

where

$$A \equiv (\delta_{jk}) - (g'_{jk}) \tag{A21}$$

Then define a sequence of vectors $\vec{f}^{(1)}$, $\vec{f}^{(2)}$, ... . The first is found by neglecting the correction term in equation A19 giving

$$\vec{f}^{(1)} = B \cdot 1 \tag{A22}$$

Then use $\vec{\vec{f}}^{(1)}$ to form the correction term and calculate an $\vec{\vec{f}}^{(2)}$ as

$$\vec{\vec{f}}^{(2)} = B \cdot \vec{\vec{\Delta}}\left(g_{jk} f_k^{(1)}\right) \tag{A23}$$

or in general

$$\vec{\vec{f}}^{(n)} = B \cdot \vec{\vec{\Delta}}\left(g_{jk} f_k^{(n-1)}\right) \qquad \text{for } n = 2, 3, 4, \ldots \tag{A24}$$

Combining these together we have

$$A \cdot \left[\vec{\vec{f}}^{(1)} + \vec{\vec{f}}^{(2)} + \ldots\right] = \vec{\vec{I}} + \vec{\vec{\Delta}}\left(g_{jk}\left(f_k^{(1)} + f_k^{(2)} + \ldots\right)\right) \tag{A25}$$

Thus, provided the sum of the $\vec{\vec{f}}^{(n)}$ converges we have

$$\vec{\vec{f}} = \sum_{n=1}^{\infty} \vec{\vec{f}}^{(n)} \tag{A26}$$

After calculating $\vec{\vec{f}}$ we calculate $\gamma$ using the Gregory integration formula on equation A5, giving

$$\gamma = 4\left\{h\left[\frac{f_1+f_N}{2} + \sum_{k=2}^{N} f_k\right] - \frac{h}{12}(\nabla f_N - \Delta f_1) - \frac{h}{24}\left(\nabla^2 f_N + \Delta^2 f_1\right)\right.$$

$$\left. - \frac{19h}{720}\left(\nabla^3 f_N - \Delta^3 f_1\right) - \ldots\right\} \tag{A27}$$

Again differences up to third order are used for the numerical calculation.

The numerical results are tabulated in table 1, including $\gamma$, $\gamma/\lambda$, and $n_s$ as functions of $\lambda$ over the range $.01 \leq \lambda \leq 100$. For comparison the asymptotic forms $\gamma_o$ and $\gamma_\infty$ are included for small $\lambda$ and large $\lambda$ respectively. For our calculations we had $N = 200$ and used the Gregory correction up to third order differences. For the matrix inversion a subroutine called MLR was used. This was written by Richard W. Sassman of Northrop Corporate Laboratories and we would like to thank him for supplying it to us.

After calculating the matrix B (for some fixed $\lambda$) the vectors $\vec{\vec{f}}^{(n)}$ were calculated for n equal to 1 through 5. The successive

corrections were most significant for the smallest $\lambda$, but for $\lambda = .01$ (the smallest $\lambda$) and N = 200 the contribution to $\gamma$ of $\vec{f}^{(5)}$ was less than about one part in $10^7$. The maximum n was taken as 5 for all the calculations.

The calculation has least accuracy for the smallest $\lambda$. This can be attributed to the larger number of correction terms required and the lower accuracy in inverting the matrix A. Note that for large $\lambda$ the diagonal terms of A are about 1 and the off-diagonal terms are of order $\lambda^{-1}$, so that A is not very much different from the identity matrix ($\delta_{jk}$) and A can be accurately inverted.

Looking at table 1a compare $\gamma$ to $\gamma_o$, the asymptotic form for small $\lambda$. $\gamma$ comes closest to $\gamma_o$ at $\lambda \simeq .012$ where they differ by about 5 parts in $10^5$. At $\lambda = .01$, the smallest $\lambda$ considered, $\gamma$ differs from $\gamma_o$ by about 5 parts in $10^4$. Now as $\gamma \to 0$ the difference $\gamma - \gamma_o$ should go to zero (by equation 38). Due to inaccuracies in the numerical calculations, however, the calculated $\gamma$ will not converge to $\gamma_o$ as $\lambda \to 0$ since one expects the errors in the numerical calculations to become worse as $\lambda \to 0$. Thus for $\lambda$ less than about .012 the asymptotic form $\gamma_o$ should be used. The relative error in the calculation of $\gamma$ is then of the order of $10^{-4}$, or even less for larger $\lambda$. For $\lambda < .01$ then $\gamma_o$ can be used with a relative error less than about $10^{-4}$.

For large $\lambda$ the table extends up to $\lambda = 100$ where $\gamma$ differs from $\gamma_\infty$ (the asymptotic form for large $\lambda$) by less than 1 part in $10^4$. Thus for $\lambda > 100$ one can use $\gamma_\infty$ with a relative error less than $10^{-4}$.

For comparison some calculations were made for small $\lambda$ with N = 150. At $\lambda = .01$ the calculated $\gamma$ differed from $\gamma_o$ by about 2 parts in $10^3$. The closest approach of $\gamma$ to $\gamma_o$ was at $\lambda \simeq .016$ where they differed by about 1 part in $10^4$. Using N = 200 then gives some improvement in accuracy for small $\lambda$.

Comparing our results with those of Cooke (reference 4), he cites Fox and Blake who found $\gamma/4 = 9.233$ for $\lambda = 0.1$. For this calculation an N of about 50 was used to obtain this 4-figure accuracy. With roundoff this agrees exactly with our result for this particular $\lambda$. Cooke also cites Nomura's results which extend down to $\lambda = 0.4$. Cooke states that he found some errors in Nomura's results in some of the points that he checked. We also find some errors in Nomura's results. Our agreement with Fox and Blake is most encouraging since the errors should increase as $\lambda$ decreases.

Another interesting result for small $\lambda$ can be found by considering $\gamma - \gamma_o$ for $.012 < \lambda < .1$. Calculating $\gamma - \gamma_o$ in this range from table 1a one notices that it roughly goes like $\lambda^2$. One might conjecture then that the asymptotic form $\gamma_o$ approximates $\gamma$ to the order of $\lambda^2$ for small $\lambda$ which would be a somewhat better

result than that proved by Hutson (equation 38). For large $\lambda$ we have shown (equation 57) that $\gamma - \gamma_\infty$ is $O(\lambda^{-2})$.

In summary, we think that over the range $.01 \leq \lambda \leq 100$ our results are accurate to about 1 part in $10^4$ or better (including the use of $\gamma_o$ for $\lambda < .012$).

| $\lambda$ | $\gamma$ | $\gamma_o$ | $\gamma/\lambda$ | $\eta_s$ |
|---|---|---|---|---|
| .010 | 321.85691 | 321.68149 | 32185.69084 | .00768 |
| .011 | 293.06271 | 293.02627 | 26642.06473 | .00847 |
| .012 | 269.15399 | 269.13933 | 22429.49909 | .00925 |
| .013 | 248.93968 | 248.92089 | 19149.20611 | .01004 |
| .014 | 231.61317 | 231.58530 | 16543.79819 | .01084 |
| .015 | 216.59354 | 216.55636 | 14439.56963 | .01163 |
| .016 | 203.44765 | 203.40186 | 12715.47791 | .01243 |
| .017 | 191.84486 | 191.79127 | 11284.99182 | .01323 |
| .018 | 181.52817 | 181.46748 | 10084.89837 | .01404 |
| .019 | 172.29468 | 172.22748 | 9068.14123 | .01485 |
| .020 | 163.98208 | 163.90884 | 8199.10381 | .01566 |
| .022 | 149.61771 | 149.53358 | 6800.80506 | .01728 |
| .024 | 137.64047 | 137.54660 | 5735.01938 | .01892 |
| .026 | 127.50009 | 127.39736 | 4903.84949 | .02057 |
| .028 | 118.80344 | 118.69251 | 4242.98010 | .02223 |
| .030 | 111.26217 | 111.14354 | 3708.73887 | .02390 |
| .032 | 104.65993 | 104.53402 | 3270.62279 | .02558 |
| .034 | 98.83127 | 98.69842 | 2906.80198 | .02726 |
| .036 | 93.64746 | 93.50794 | 2601.31820 | .02896 |
| .038 | 89.00684 | 88.86091 | 2342.28539 | .03067 |
| .040 | 84.82810 | 84.67594 | 2120.70249 | .03238 |
| .042 | 81.04536 | 80.88717 | 1929.65145 | .03411 |
| .044 | 77.60473 | 77.44066 | 1763.74393 | .03584 |
| .046 | 74.46168 | 74.29187 | 1618.73222 | .03759 |
| .048 | 71.57909 | 71.40366 | 1491.23106 | .03934 |
| .050 | 68.92577 | 68.74485 | 1378.51546 | .04110 |
| .055 | 63.13177 | 62.93756 | 1147.85042 | .04554 |
| .060 | 58.29752 | 58.09056 | 971.62535 | .05004 |
| .065 | 54.20208 | 53.98284 | 833.87814 | .05458 |
| .070 | 50.68755 | 50.45643 | 724.10790 | .05918 |
| .075 | 47.63809 | 47.39545 | 635.17457 | .06384 |
| .080 | 44.96677 | 44.71292 | 562.08461 | .06854 |
| .085 | 42.60707 | 42.34230 | 501.25965 | .07329 |
| .090 | 40.50724 | 40.23182 | 450.08047 | .07809 |
| .095 | 38.62640 | 38.34056 | 406.59373 | .08294 |
| .100 | 36.93184 | 36.63580 | 369.31836 | .08784 |

Table 1a. Normalized Capacitance and Figure of Merit

| $\lambda$ | $\gamma$ | $\gamma_o$ | $\gamma/\lambda$ | $\eta_s$ |
|---|---|---|---|---|
| .10 | 36.93184 | 36.63580 | 369.31836 | .08784 |
| .11 | 34.00031 | 33.68450 | 309.09374 | .09777 |
| .12 | 31.55236 | 31.21750 | 262.93630 | .10789 |
| .13 | 29.47687 | 29.12362 | 226.74519 | .11818 |
| .14 | 27.69444 | 27.32336 | 197.81740 | .12864 |
| .15 | 26.14674 | 25.75837 | 174.31159 | .13927 |
| .16 | 24.79001 | 24.38484 | 154.93758 | .15006 |
| .17 | 23.59076 | 23.16922 | 138.76916 | .16101 |
| .18 | 22.52289 | 22.08539 | 125.12717 | .17212 |
| .19 | 21.56580 | 21.11273 | 113.50423 | .18337 |
| .20 | 20.70300 | 20.23471 | 103.51498 | .19477 |
| .22 | 19.20916 | 18.71140 | 87.31435 | .21799 |
| .24 | 17.96044 | 17.43439 | 74.83517 | .24173 |
| .26 | 16.90072 | 16.34743 | 65.00277 | .26598 |
| .28 | 15.98984 | 15.41025 | 57.10656 | .29069 |
| .30 | 15.19829 | 14.59326 | 50.66096 | .31583 |
| .32 | 14.50391 | 13.87422 | 45.32472 | .34137 |
| .34 | 13.88972 | 13.23610 | 40.85213 | .36729 |
| .36 | 13.34251 | 12.66561 | 37.06253 | .39353 |
| .38 | 12.85180 | 12.15224 | 33.82054 | .42009 |
| .40 | 12.40923 | 11.68758 | 31.02307 | .44692 |
| .42 | 12.00799 | 11.26479 | 28.59045 | .47399 |
| .44 | 11.64252 | 10.87828 | 26.46027 | .50127 |
| .46 | 11.30821 | 10.52339 | 24.58307 | .52874 |
| .48 | 11.00122 | 10.19627 | 22.91920 | .55636 |
| .50 | 10.71831 | 9.89364 | 21.43662 | .58410 |
| .55 | 10.09939 | 9.22714 | 18.36252 | .65379 |
| .60 | 9.58177 | 8.66413 | 15.96962 | .72364 |
| .65 | 9.14241 | 8.18132 | 14.06525 | .79321 |
| .70 | 8.76478 | 7.76198 | 12.52112 | .86212 |
| .75 | 8.43672 | 7.39379 | 11.24896 | .93002 |
| .80 | 8.14908 | 7.06745 | 10.18635 | .99658 |
| .85 | 7.89483 | 6.77582 | 9.28804 | 1.06151 |
| .90 | 7.66851 | 6.51333 | 8.52057 | 1.12455 |
| .95 | 7.46578 | 6.27555 | 7.85871 | 1.18549 |
| 1.00 | 7.28315 | 6.05891 | 7.28315 | 1.24413 |

Table 1b. Normalized Capacitance and Figure of Merit

| $\lambda$ | $\gamma$ | $\gamma_\infty$ | $\gamma/\lambda$ | $\eta_s$ |
|---|---|---|---|---|
| 1.0 | 7.28315 | 6.54648 | 7.28315 | 1.24413 |
| 1.1 | 6.96742 | 6.31498 | 6.33401 | 1.35395 |
| 1.2 | 6.70418 | 6.12207 | 5.58681 | 1.45315 |
| 1.3 | 6.48150 | 5.95883 | 4.98577 | 1.54133 |
| 1.4 | 6.29080 | 5.81892 | 4.49343 | 1.61843 |
| 1.5 | 6.12578 | 5.69765 | 4.08385 | 1.68471 |
| 1.6 | 5.98168 | 5.59155 | 3.73855 | 1.74064 |
| 1.7 | 5.85483 | 5.49793 | 3.44402 | 1.78684 |
| 1.8 | 5.74239 | 5.41471 | 3.19021 | 1.82403 |
| 1.9 | 5.64209 | 5.34025 | 2.96952 | 1.85298 |
| 2.0 | 5.55211 | 5.27324 | 2.77606 | 1.87450 |
| 2.2 | 5.39751 | 5.15749 | 2.45341 | 1.89829 |
| 2.4 | 5.26963 | 5.06103 | 2.19568 | 1.90121 |
| 2.6 | 5.16226 | 4.97942 | 1.98548 | 1.88830 |
| 2.8 | 5.07095 | 4.90946 | 1.81105 | 1.86372 |
| 3.0 | 4.99243 | 4.84883 | 1.66414 | 1.83080 |
| 3.2 | 4.92425 | 4.79578 | 1.53883 | 1.79216 |
| 3.4 | 4.86455 | 4.74897 | 1.43075 | 1.74980 |
| 3.6 | 4.81186 | 4.70736 | 1.33663 | 1.70522 |
| 3.8 | 4.76505 | 4.67013 | 1.25396 | 1.65957 |
| 4.0 | 4.72320 | 4.63662 | 1.18080 | 1.61366 |
| 4.2 | 4.68558 | 4.60631 | 1.11561 | 1.56811 |
| 4.4 | 4.65159 | 4.57875 | 1.05718 | 1.52335 |
| 4.6 | 4.62074 | 4.55358 | 1.00451 | 1.47966 |
| 4.8 | 4.59262 | 4.53052 | .95680 | 1.43726 |
| 5.0 | 4.56689 | 4.50930 | .91338 | 1.39626 |
| 5.5 | 4.51124 | 4.46300 | .82023 | 1.30027 |
| 6.0 | 4.46539 | 4.42441 | .74423 | 1.21359 |
| 6.5 | 4.42699 | 4.39177 | .68108 | 1.13572 |
| 7.0 | 4.39438 | 4.36378 | .62777 | 1.06582 |
| 7.5 | 4.36636 | 4.33953 | .58218 | 1.00302 |
| 8.0 | 4.34202 | 4.31831 | .54275 | .94648 |
| 8.5 | 4.32068 | 4.29959 | .50832 | .89543 |
| 9.0 | 4.30184 | 4.28294 | .47798 | .84920 |
| 9.5 | 4.28507 | 4.26805 | .45106 | .80721 |
| 10.0 | 4.27006 | 4.25465 | .42701 | .76893 |

Table 1c. Normalized Capacitance and Figure of Merit

| $\lambda$ | $\gamma$ | $\gamma_\infty$ | $\gamma/\lambda$ | $\eta_s$ |
|---|---|---|---|---|
| 10. | 4.27006 | 4.25465 | .42701 | .76893 |
| 11. | 4.24430 | 4.23150 | .38585 | .70182 |
| 12. | 4.23301 | 4.21221 | .35192 | .64505 |
| 13. | 4.20512 | 4.19588 | .32347 | .59648 |
| 14. | 4.18988 | 4.18189 | .29928 | .55452 |
| 15. | 4.17675 | 4.16977 | .27845 | .51793 |
| 16. | 4.16530 | 4.15916 | .26033 | .48577 |
| 17. | 4.15525 | 4.14979 | .24443 | .45729 |
| 18. | 4.14635 | 4.14147 | .23035 | .43192 |
| 19. | 4.13841 | 4.13403 | .21781 | .40917 |
| 20. | 4.13128 | 4.12732 | .20656 | .38866 |
| 22. | 4.11903 | 4.11575 | .18723 | .35319 |
| 24. | 4.10887 | 4.10610 | .17120 | .32360 |
| 26. | 4.10030 | 4.09794 | .15770 | .29854 |
| 28. | 4.09298 | 4.09095 | .14618 | .27706 |
| 30. | 4.08666 | 4.08488 | .13622 | .25844 |
| 32. | 4.08114 | 4.07958 | .12754 | .24215 |
| 34. | 4.07628 | 4.07490 | .11989 | .22779 |
| 36. | 4.07197 | 4.07074 | .11311 | .21503 |
| 38. | 4.06812 | 4.06701 | .10706 | .20362 |
| 40. | 4.06466 | 4.06366 | .10162 | .19335 |
| 42. | 4.06154 | 4.06063 | .09670 | .18406 |
| 44. | 4.05870 | 4.05787 | .09224 | .17563 |
| 46. | 4.05612 | 4.05536 | .08818 | .16793 |
| 48. | 4.05375 | 4.05305 | .08445 | .16087 |
| 50. | 4.05157 | 4.05093 | .08103 | .15439 |
| 55. | 4.04683 | 4.04630 | .07358 | .14025 |
| 60. | 4.04289 | 4.04244 | .06738 | .12848 |
| 65. | 4.03956 | 4.03918 | .06215 | .11852 |
| 70. | 4.03671 | 4.03638 | .05767 | .11000 |
| 75. | 4.03424 | 4.03395 | .05379 | .10262 |
| 80. | 4.03208 | 4.03183 | .05040 | .09617 |
| 85. | 4.03018 | 4.02996 | .04741 | .09048 |
| 90. | 4.02849 | 4.02829 | .04476 | .08542 |
| 95. | 4.02698 | 4.02681 | .04239 | .08090 |
| 100. | 4.02563 | 4.02546 | .04026 | .07684 |

Table 1d. Normalized Capacitance and Figure of Merit